Biochimica et Biophysica Acta 1818 (2012) 12–18

Contents lists available at SciVerse ScienceDirect

Biochimica et Biophysica Acta

journal homepage: www.elsevier.com/locate/bbamem

Caveolin-1 hydrophobic segment peptides insertion into membrane mimetic systems: Role of Proline residue

Satoko Aoki, Richard M. Epand *

Department of Biochemistry and Biomedical Sciences, McMaster University Health Science Center, Hamilton, Ontario, Canada L8S 4K1

ARTICLE INFO

Article history:
Received 28 April 2011
Received in revised form 8 September 2011
Accepted 11 September 2011
Available online 17 September 2011

Keywords:
Caveolin-1
Hydrophobic segment
Monotopic protein
Re-entrant helix
Transmembrane helix

ABSTRACT

Caveolin-1 has a segment of hydrophobic amino acids comprising approximately residues 103–122 that are anchored to the membrane with cholesterol-rich domains. Previously, we reported that changing the Pro^{110} residue to Ala (the P110A mutant) prevents not only the localization of the protein into lipid rafts but also the formation and functioning of caveolae. The conformational state of caveolin-1 can be shifted toward the transmembrane arrangement by this single amino acid mutation. To model the conformation, and extent of membrane insertion of this segment into membrane-mimetic environments, we have prepared a peptide corresponding to this hydrophobic segment of caveolin-1 having the sequence KKKKLSTIFGIPMALIWGIY-FAILKKKKK-amide and the mutated version, KKKKLSTIFGIAMALIWGIYFAILKKKKK-amide. These peptides contain flanking Lys residues to facilitate purification and handling of the peptide. Circular dichroism measurements demonstrated that the mutated peptide has increased helical content compared with the wild type both in the presence and absence of lipid. The fluorescence emission from the Trp residues in the peptide showed significant blue shifts in the presence of liposomes, however the presence of cholesterol in hydrated vesicle bilayers decreases its helical content. Our overall findings support our studies with the intact protein in cells and suggest that the peptide of WT caveolin-1 hydrophobic segment has an intrinsic preference not to maintain its conformation as a rigid transmembrane helix. Substituting the Pro residue with an Ala allows the peptide to exist in a more hydrophobic environment likely as a consequence of a change in its conformation to a straight hydrophobic helix that traverses the membrane.

1. Introduction

Caveolae are sphingomyelin and cholesterol rich invaginations (50–100 nm diameter) in the plasma membrane, that bud inward toward the cell [1]. They appear to have a number of functions, including roles in signal transduction [2,3], calcium signaling [4,5], lipid recycling [6,7] and membrane traffic [1]. Caveolae are particularly prevalent in adipocytes, endothelial cells and myocytes. EGF receptor, PDGF receptor, membrane estrogen receptor, H-Ras, and extracellular signal regulated kinase (ERK-1/2), appear to be regulated by their interaction with caveolae [8–10]. Caveolae and their constituent proteins, caveolins, have a critical role in cardiovascular function, including regulation of cholesterol metabolism, nitric oxide synthesis and cardiac function [11]. Caveolin-1 has also been hypothesized to be an intensive tumor suppressor, since sporadic mutations of caveolin-1 have been found in many human cancers [12]. In contrast, caveolin-1 may work as a tumor promoter in prostate cancer [13]. The involvement of caveolae in a wide range of disease processes has been suggested [14–17].

One of the features of caveolae is the presence of several forms of the protein caveolin [18,19]. Caveolin-1 structure has not yet been resolved by crystallographic analysis. Most experimental evidence indicates that the membrane-inserting segment of caveolin-1 forms a U-shaped structure within the membrane having both the N-terminal and C-terminal domains on the cytoplasmic side of the plasma membrane [20]. Caveolin-1 is anchored to the membrane with three palmitoyl chains attached to Cys residues as well as with a hydrophobic segment comprising residues 103–122 [21]. A similar segment comprising residues 102–134 had been previous proposed as the membrane insertion segment [20]. The protein inserts into membranes of phosphatidylcholine in a cholesterol-dependent manner [22]. This hydrophobic segment is thought to form a U-shaped, re-entrant helix rather than a transmembrane helix

Abbreviations: DPPC, 1,2-dipalmitoyl-sn-glycero-3-phosphocholine; F_0, maximum fluorescence emission intensity without quencher; F, and maximum fluorescence emission intensity with the quencher; K_{SV}, Stern–Volmer quenching constant; LPC, Lysophosphatidylcholine (the 1-palmitoyl form); P110A, the peptide KKKKLSTIFGIA-MALIWGIYFAILKKKKK-amide; PO/DP/Ch, equimolar mixture of POPC, DPPC and cholesterol; POPC, 1-palmitoyl-2-oleoyl-sn-glycero-3-phosphocholine; SUV, small unilamellar vesicle; WT, the peptide KKKKLSTIFGIPMALIWGIYFAILKKKKK-amide

* Corresponding author at: Department of Biochemistry and Biomedical Sciences, McMaster University Health Science Center, Hamilton, Ontario, Canada L8S 4K1. Tel.: +1 905 525 9140x22073; fax: +1 905 521 1397.
E-mail address: epand@mcmaster.ca (R.M. Epand).

0005-2736/$ – see front matter © 2011 Elsevier B.V. All rights reserved.
doi:10.1016/j.bbamem.2011.09.009

[19,23,24]. The hydrophobic segment of caveolin-1 is a well conserved region in evolution, suggesting that this segment plays an important role for caveolin-1 function.

In silico modeling predicts that substituting the Pro^{110} residue of caveolin-1 with an Ala will change the conformation to a straight helix that would traverse the membrane. Furthermore, we found that the substitution of Pro^{110} with an Ala influenced the ability of caveolae to be endocytosed, and to form lipid droplets indicating that the multiple activities of caveolin-1 are a consequence of the topology- and compartment-specific cellular localization of this protein [21]. In the present study we investigate if the structural preferences of the isolated hydrophobic segment are responsible for the drastic topological change caused by this single Pro mutation. We analyzed the structural tendency of model peptides corresponding to the caveolin-1 hydrophobic segment and a mutant form, using tryptophan fluorescence and circular dichroism in the presence and absence of lipids. The results provide insights into the functional importance of this segment in intact caveolin-1 and the role of its Pro residue.

2. Materials and methods

2.1. Materials

LPC, POPC, DPPC and Cholesterol were obtained from Avanti Polar Lipids (AL, USA). Acrylamide was purchased from Life Technologies (MD, USA). Chloroform and Methanol were obtained from CALEDON (ON, Canada). The stock solution of acrylamide (Life Technologies Inc. MD, USA) was 5 M in ddH_2O. Buffers were filtered through an Acrodisc Syringe Filter (0.2 μm pore size; PALL). Peptides corresponding to the caveolin-1 wild type hydrophobic segment: L103–L122 (WT) and the mutated version of this peptide: L103–P110A–L122 (P110A) were synthesized by SynBioSci (CA, USA), with four Lys residues on the C-terminus, five Lys residues on the N-terminus and amidated at the C-terminus. The sequences of the two peptides were: KKKKLSTIFGIPMALIWGIYFAILKKKKK-amide and the mutated version, KKKKLSTIFGIAMALIWGIYFAILKKKKK-amide. Peptides were dissolved in 5 mM Hepes buffer, pH 7.4, 50 mM NaCl (HEPES buffer) at a concentration of 1 mg/ml. The exact concentration was determined by absorbance measurements at 280 nm using molar extinction coefficients based on the Trp and Tyr content of the peptides.

2.2. Preparation of phospholipid small unilamellar vesicles (SUVs)

The desired amount of lipids were dissolved in chloroform and methanol, 2:1 (v/v), and dried in glass tubes under nitrogen, and followed by vacuum for 3 h. Lipid suspensions were prepared by vortex mixing in HEPES buffer. The lipid films were suspended in buffer at room temperature. Sonication of lipid dispersions was performed in 5 ml glass tubes in a bath-type sonicator (Model 08849–00, Cole-Parmer Instrument Company, IL, USA) for 5 min (until clear). To avoid degradation of lipids, sonication was performed at ~10 °C under a nitrogen atmosphere. Vesicles were used on the day of preparation.

2.3. Fluorescence titration measurements

Peptide and lipid interactions were studied by monitoring the changes in the Trp fluorescence emission spectra of the peptides upon addition of SUVs [25,26]. Intrinsic fluorescence of the Trp residues was measured using 5 μM solutions of the WT and P110A peptides in HEPES buffer or after addition of different amounts of lipid vesicles. Trp fluorescence was measured using a quartz microplate at 25 °C in a monochromator-based microplate fluorimetry (TECAN SAFAIRE, Tecan Group Ltd., Männedorf, Switzerland). Excitation wavelength was 295 nm, and emission spectra were recorded from 305 to 450 nm (5 mm excitation bandwidth and 5 mm emission bandwidth). Spectra were collected with a step size of 1 nm. All measurements were corrected for light scattering effects by subtraction of background. Background samples were prepared using the same protocol except HEPES buffer instead of peptide solution was added. Blue shifts were calculated as the difference in the wavelength of the maximal emission of the peptide with or without lipid. 5 μM peptides were used in 200 μM total lipid concentration giving a maximal lipid-to-peptide ratio of 40.

The extent of peptide burial in the lipid bilayer was determined from the intrinsic Trp fluorescence intensity of the peptides in the presence and absence of SUVs [27–29]. The maximal fluorescence emission intensity of the peptide was plotted against the added lipid concentration [30–32]. Data were smoothed by the Adjacent Averaging method to the original fluorescence spectra using Origin 5.0 software.

2.4. Quenching experiments

Peptide and lipid interactions are accompanied by changes in the accessibility of the peptides to aqueous quenchers of Trp fluorescence in the presence of SUVs [33]. Acrylamide quenching experiments were carried out using a 5 μM peptide solution in the absence or presence of SUVs by addition of aliquots of varying concentrations of acrylamide [25,26]. Samples were freshly prepared in HEPES buffer. The lipid and peptide mixtures (molar ratio of 40:1) were incubated for 1 h at room temperature prior to the measurements. The excitation wavelength was set at 295 nm instead of 280 nm to reduce the absorbance by acrylamide and the inner filter effect. The emission spectra were recorded between 300 and 450 nm after addition of quencher at 25 °C, followed by spectral correction by subtracting the spectra measured under identical conditions but without the peptide. The maximum fluorescence intensities without and with the quencher (F_0 and F respectively) were determined, and F_0/F values were plotted against the acrylamide concentration. The slopes of the best-fit linear plots were used to determine the Stern–Volmer quenching constants (K_{SV}). The experimental data were analyzed according to the Stern–Volmer equation [34]

$$(F_0/F) = 1 + K_{SV}[Q]. \quad (1)$$

Data were smoothed by the Adjacent Averaging method to original fluorescence spectra using Origin 5.0 software.

2.5. Circular dichroism (CD) spectroscopy

Circular dichroism spectra were collected using a Circular Dichroism Spectrometer Model 410 (Aviv Biomedical Inc., NJ, USA). Spectral scans were performed from 260 to 195 nm, with step resolution of 1.0 nm and bandwidth of 1.0 nm. A 1-mm-path-length quartz cuvette was used for the measurements. Freshly prepared samples were measured at a peptide concentration of 50 μM in HEPES buffer. The secondary structure of the peptides was determined by applying the Adjacent Averaging method to the original spectra using the Origin 5.0 software and was analyzed by the CDPro program.

2.6. Reproducibility of spectral measurements

The fluorescence and CD measurements were repeated at least once, giving similar results. A representative set of data, run at the same time, is presented. We did not undertake a detailed statistical analysis of the error because the properties of the two peptides were generally qualitatively different and showed a 1.7–2.9 fold difference.

3. Results

3.1. Peptide design

A model peptide was designed to correspond to the hydrophobic segment of the mouse caveolin-1 sequence L103–L122. The mean

hydrophobicity of WT and P110A are 4.24 and 5.03 respectively (ANTHEPROT 2000V6.0 release 1.1.54) [35]. According to 'Lys-tagging' guidelines for synthesis of hydrophobic peptides [36,37], a total of nine Lys residues were attached to the hydrophobic core sequence of L103–L122 to produce a water-soluble product. The resulting peptide, designated WT has the sequence KKKK-LSTIFGIPMALIWGIYFAIL-KKKKK. We also prepared a mutated version of this peptide, designed P110A, with the sequence KKKK-LSTIFGIAMALIWGIYFAIL-KKKKK. Consistent with previous applications of this hydrophilic tagging approach, we recognized that the peptide designed in this manner had the beneficial attributes of water solubility and ease of purification [36,38,39]. Previous studies showed that the addition of Lys to hydrophobic peptides does not prevent them from adopting a stable α-helical conformation both in solution and in lipid bilayers, furthermore, the number of Lys residues added does not affect peptide tertiary packing [40–43].

3.2. Fluorescence properties of the WT and P110A peptides in buffer

The fluorescence emission of the two model peptides was measured as a function of peptide concentration in buffer (Fig. 1a). It was found that the emission intensity was proportional to the peptide concentration for both peptides (Fig. 1b). This indicates that in buffer the peptides do not undergo a self-association process that affects the environment of the Trp residues. In addition, the proportionality between fluorescence emission intensity and peptide concentration demonstrates the lack of significant inner filter effects. The fluorescence emission intensity is greater for the P110A compared with the WT (Fig. 1). In addition, the wavelength of maximal emission is shifted 8 nm to lower wavelengths for the P110A peptide compared with the WT peptide (Fig. 1a). Both the increased emission intensity and lower fluorescence emission maximum of the P110A indicate that its Trp residue is in a more hydrophobic environment, even for the peptide in buffer without the addition of lipid.

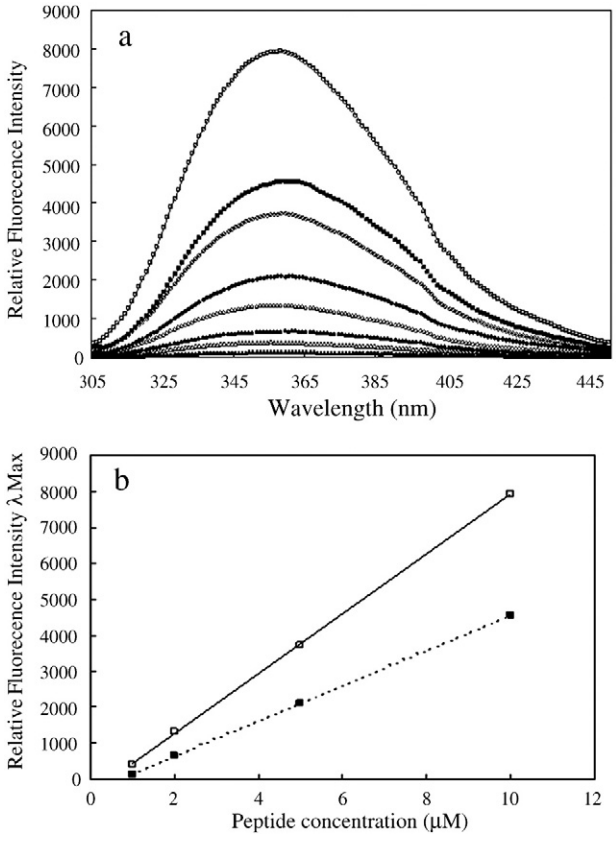

Fig. 1. Fluorescence emission spectra of peptides. (a) Fluorescence emission spectra of WT and P110A in buffer. Peptides concentration was adjusted for 10 μM (WT: ■, P110A: □), 5 μM (WT: ◆, P110A: ◇), 2 μM (WT: ●, P110A: ○), 1 μM (WT: ▲, P110A: △). (b) Relative fluorescence intensity at λ_{max} against peptide concentration (WT: ■, P110A: □). A representative experiment is shown that was repeated twice. Wavelength accuracy is ±1 nm. The regression coefficients were 0.99 for both WT and P110A.

3.3. Fluorescence properties of the WT and P110A peptides in the presence of lipids

Measurements of fluorescence emission intensity and shifts in the λ_{max} of two Trp residues naturally contained in the hydrophobic core of the peptide are particularly useful for analysis of the insertion/positioning of either WT or P110A within the membrane [36,44]. In order to compare the properties of the peptides in different lipid environments, we used a range of lipid to peptide molar ratios to assure that sufficient SUVs of POPC or a micellar solution of LPC were used to cause all of the peptide to translocate to the lipid (Fig. 2). Cholesterol was also included in one set of SUVs with the composition PO/DP/Ch, (molar ratio of 1:1:1). The Trp fluorescence emission spectra of either WT or P110A were measured either in buffer or in the presence of SUVs and are shown on Fig. 2 at 10:1, 20:1, 40:1 and 80:1 lipid-to-peptide molar ratios. For all of the peptides and with all of the lipid mixtures used, an increase in the Lipid/Peptide ratio resulted in an increase in the intensity of the fluorescence emission. The only exception to this was the wild type peptide in the presence of SUVs composed of PO/DP/Ch (Fig. 2, panel a-3). In this case increase in lipid concentration resulted in a decrease in the magnitude of fluorescence emission. This may be caused by the lipid causing quenching of the Trp fluorescence or as a result of these SUVs causing more scattering and lowering the intensity of both the excitation and emission beams. The corresponding titration curves were obtained for either WT or P110A by plotting either the maximal Trp emission wavelength (λ_{max}) (Fig. 2b-1) or the fluorescence intensity at λ_{max} (Fig. 2 b-2). In the experiments with SUVs composed of POPC, the P110A peptide shifted the emission λ_{max} to lower wavelengths, by 8 nm at higher lipid concentrations (Fig. 2, a-2, b-1). This shift was accompanied by an enhancement of the emission intensity (Fig. 2, b-2). In contrast, the blue shift of WT was only 2 nm with POPC at higher peptide concentrations (Fig. 2, b-1). These results provide evidence of insertion of the P110A into non-polar environments [44] corresponding to deeper insertion into the membrane than WT. We also observed a decrease in the blue shift upon addition of cholesterol to SUVs composed of POPC/DPPC for both WT and P110A (Fig. 2, b-1). Addition of LPC increased the Trp fluorescence intensity for P110A more than that for WT (Fig. 2, b-2), but it did not affect λ_{max}. This indicated that P110A was more protected from collisional quenching by the micelle than WT, suggesting the greater penetration of P110A into the micelle. However, the lack of effect of LPC on the emission maximum of either peptide indicates that a membrane bilayer environment and not in a micelle is required to increase the hydrophobicity of the environment of the Trp in P110A.

Additional support for the transfer of Trp of WT and the P110A from the aqueous to the membrane environment was obtained from Trp fluorescence quenching by a water-soluble quencher, acrylamide [25,26]. Stern–Volmer plots of acrylamide quenching are shown in Fig. 3, for WT and P110A in buffer and in the presence of SUVs composed of POPC or PO/DP/Ch. The calculated Stern–Volmer constants (K_{sv}) are summarized in Table 1. The Stern–Volmer constant (K_{sv}) is a measure of the efficiency of fluorescence quenching. The two peptides have similar quenching constants in buffer but the addition of SUVs of POPC greatly reduces the extent of acrylamide quenching. This protection by the lipid is somewhat greater for the P110A than for WT again indicating the greater depth of insertion of P110A into the membrane. Surprisingly SUVs composed of PO/DP/Ch increase the quenching of WT. This may reflect a greater static quenching component of this peptide in buffer. For both peptides, the lipid mixture PO/DP/Ch contributes little protection against quenching, suggesting that cholesterol inhibits penetration of the peptide into the membrane.

3.4. Helicity of either WT or P110A peptide in membrane environments

The CD spectra of either WT or P110A were measured in the presence and absence of two SUVs having two different lipid compositions, as well as with LPC micelles (Fig. 4, Table 2). All of the samples were not turbid and were visually transparent. Changes in the CD properties of the peptides caused by the addition of SUVs were compared with the effects of LPC micelles. The LPC micelles are much smaller than SUVs and consequently do not exhibit light scattering artifacts [45–49]. The CD spectrum of P110A in buffer, SUVs of POPC or SUV-PO/DP/Ch displayed a positive maximum at ~195 nm and double minima at ~208 and ~222 nm, indicative of some α-helical character [50]. The addition of SUVs of POPC caused an increase in the intensity of these maximum and minimum ellipticities, indicative of higher helical content, as confirmed by deconvolution of the CD spectra (Table 2). The addition of SUVs composed of PO/DP/Ch decreased in the intensity of these maximum and minimum ellipticities suggesting that peptide insertion into the bilayer was inhibited by the presence of cholesterol that caused tighter packing of the lipid. Percentages of α-helical structure of the P110A in buffer or in the presence of SUVs of POPC are approximately 1.5–2 times higher than those of WT. In the presence of SUVs of PO/DP/Ch, likely due to the presence of cholesterol, the insertion of peptide into SUVs was inhibited and the percentages of α-helical structure of P110A were smaller. The fraction of α-helical structure found in the presence of LPC (Table 2) was much greater for LPC than for the SUVs. The LPC provides a loose environment into which the peptide can penetrate better than the tight packing of the either POPC or PO/DP/Ch bilayer. Therefore, the bilayer would prevent complete insertion of the peptide and make it more difficult to form a full alpha-helix, while with LPC and the peptide can mix better resulting in more alpha-helix. In addition, the lack of light scattering artifacts with LPC may contribute to this increase.

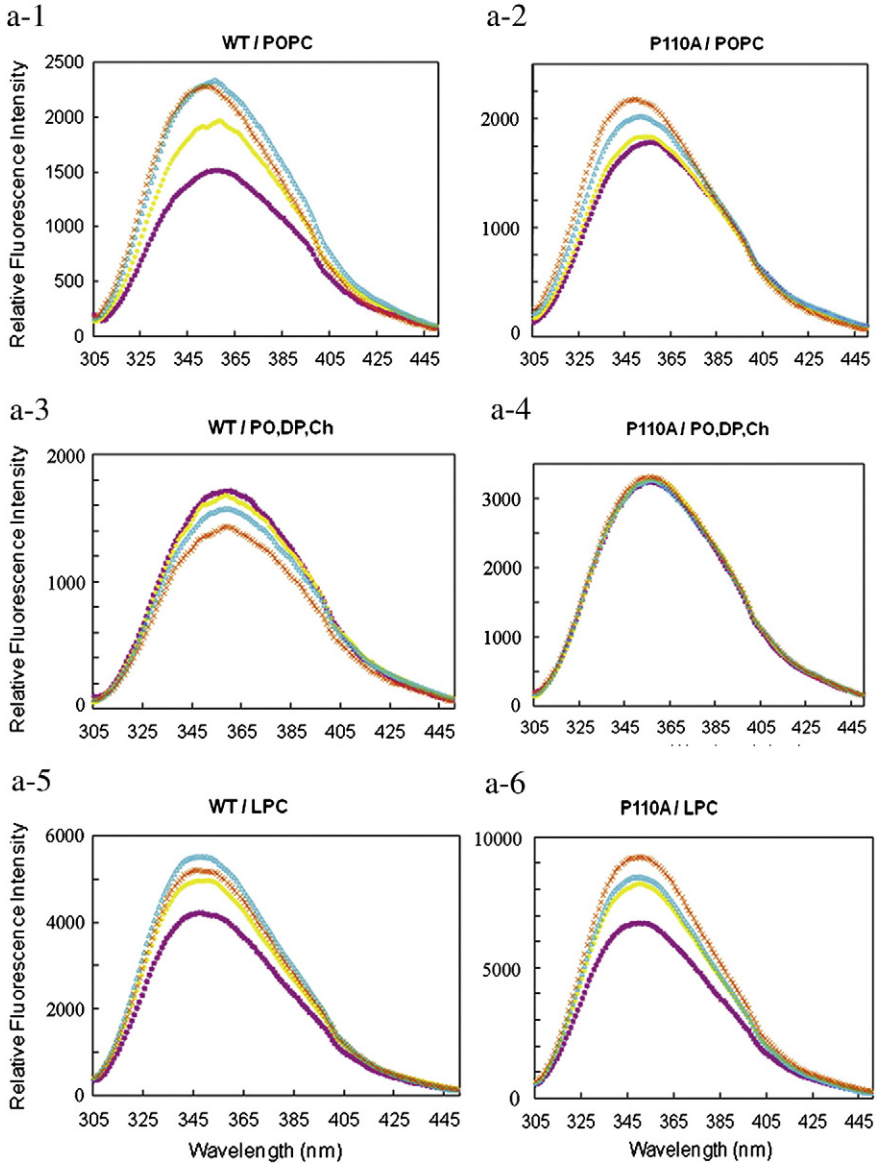

Fig. 2. Fluorescence emission spectra and titration curves of peptides with lipids. (a) Fluorescence emission spectra of either WT (a-1, 3, 5) or P110A (a-2, 4, 6) peptides with different lipid SUVs; POPC (a-1, 2), PO/DP/Ch (a-3, 4) and micelle LPC (a-5, 6). The lipid to peptide ratios were 10 (+, purple), 20 (◇, yellow), 40 (▲, blue) and 80 (x, orange). Peptide concentration was 5 μM. (b) Shift in the (b-1): wavelength of maximal Trp emission wavelength (λ_{max}) and (b-2): the fluorescence intensity at λ_{max} relative to the value measured for a sample with a Lipid: Peptide = 1:10. Peptides with different SUVs: POPC (WT: ■, P110A: □); PO/DP/Ch (WT: ♦, P110A: X); LPC (WT: ●, P110A: ○). A representative experiment is shown that was repeated twice. Wavelength accuracy is ± 1 nm.

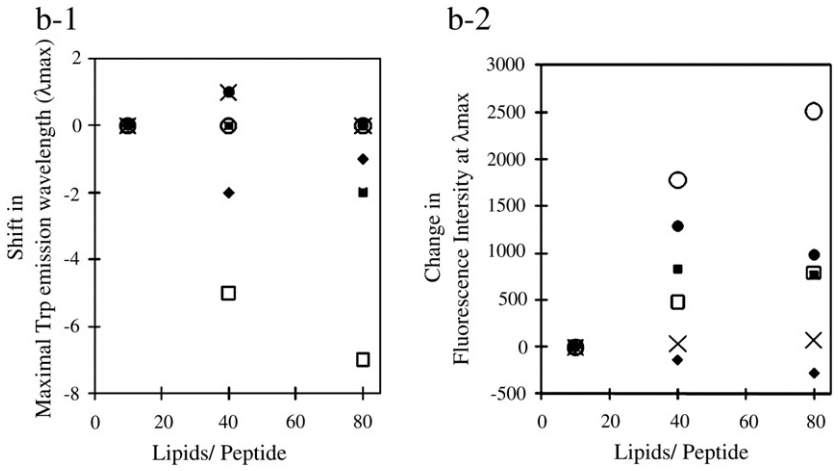

Fig. 2 (*continued*).

4. Discussion

Caveolin, a 22–24 kDa protein, is an integral membrane protein component of caveolae membranes. The major lipid components of caveolae domains are sphingomyelin, phosphatidylcholine and cholesterol [51]. Many aspects of the hydrophobic segment of caveolin-1, which is anchored to the membrane by forming a re-entrant helix, have been studied [22,52–54]. There are several reports about caveolin-1 being recruited to cholesterol-rich lipid raft domains of membranes. Cholesterol might increase the thickness of the membrane to accommodate the exact lipid environment for incorporation of caveolin or it might interact with caveolin directly. Research using model peptides indicated that a segment with the sequence VTKYWFYR that corresponds to a CRAC motif constituting residues 94–101 (human), promotes the formation of cholesterol rich domains [54]. This CRAC domain is outside of the hydrophobic segment studied in the present work. In addition, studies with caveolin-1 mutants indicate that the segment of residues 82–101 (human) has an important role for membrane binding and has been called the scaffolding domain [23]. Another feature of the interaction of caveolin with membranes is that the hydrophobic segment studied in the present work is thought to form a U-shaped, re-entrant helix. In our previous study, we focused on this hydrophobic segment in the intact caveolin. We reported that membrane topology of the hydrophobic segment is altered as a consequence of a P110A mutation to become transmembrane. This change in membrane topology of the protein prevents not only the localization of caveolin-1 into cholesterol-rich lipid rafts but also caveolae formation and functions [21].

The present study was aimed at getting better insight into the contribution of the Pro residue of the isolated hydrophobic segment of caveolin-1 by the interaction of model peptides and cell membrane-mimicking phospholipid vesicles. We investigated the fluorescence properties of the wild type form of this peptide, WT, as well as a corresponding peptide, P110A, with an Ala substituting for Pro. For WT and P110A in a buffer environment, the Trp residues are highly exposed to the solvent. Addition of SUVs of POPC results in greater burial of the Trp of the P110A compared with WT as shown both by the change in emission maximum as well as a greater decrease in acrylamide quenching. These effects were much less using SUVs of PO/DP/Ch, suggesting that cholesterol may inhibit penetration of the peptides into the bilayer. This would suggest that in a cholesterol-rich domain of a biological membrane this hydrophobic segment would not penetrate deeply into the bilayer. These changes in Trp fluorescence were in accord with CD measurements that also indicated greater increases in helicity of the P110A compared with WT upon addition of lipid and lesser effects when cholesterol was added. In addition, one of the interesting findings is the observation that the Trp residue in the P110A peptide was sequestered in a more hydrophobic environment than that of the WT in buffer. The process whereby re-entrant loops partition into the membrane is largely uncharacterized, and it is not beyond the scope of possibility that a pre-formed structure in aqueous media might facilitate membrane insertion. Such a preformed structure for the P110A mutant in aqueous media is supported by the fluorescence results (Fig. 1).

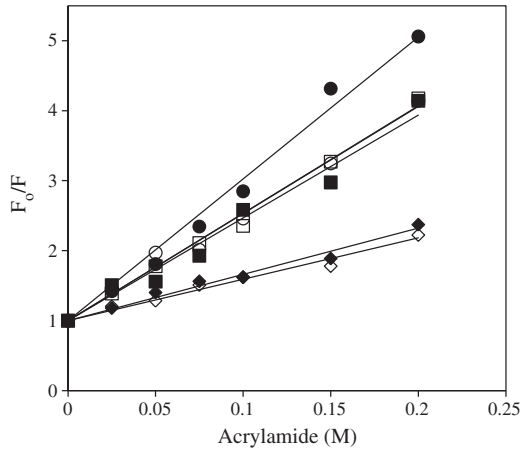

Fig. 3. Stern–Volmer plots for acrylamide quenching of the Trp fluorescence of the peptides. Peptides in buffer (WT: ■, P110A: □), and in the presence of SUVs composed of POPC (WT: ◆, P110A: ◇) and PO/DP/Ch (WT: ●, P110A: ○). Lipids and peptide concentration were, respectively, 200 μM and 5 μM. Linear trend lines were added. This is representative data from experiments repeated twice.

Table 1
Stern–Volmer constants K_{sv} for fluorescence emission quenching of Trp residues in either WT or P110A peptide incubation with SUVs. PO, POPC; DP, DPPC; Ch, Cholesterol. A representative experiment is shown that was repeated twice. Wavelength accuracy for Absorbance/Fluorescence is ±1 nm. Stern–Volmer constants K_{sv} for fluorescence emission quenching of Trp residues.

Lipids	Stern–Volmer constant K_{sv} (M^{-1})	
	WT	P110A
(Buffer)	14.7	15.3
POPC	6.6	5.9
PO,DP,Ch	20.3	15.3

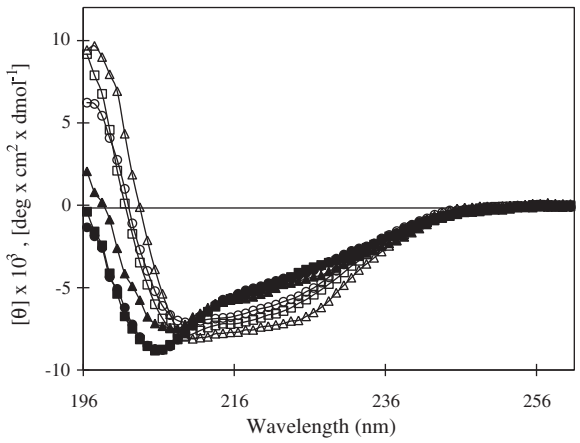

Fig. 4. Circular dichroism spectra of peptides. Peptides in buffer (WT: ■, P110A: □), in the presence of SUVs consisting of POPC (WT: ▲, P110A: △) or of PO/DP/Ch (WT: ●, P110A: ○). Peptide concentration was 50 μM (0.15 mg/ml in buffer), lipid concentration was 1 mM. This is representative data from experiments repeated twice.

In summary, this research suggests that the conformational state of the P110A caveolin-1 hydrophobic segment – flanked by Lys tags – inserts deeply into bilayer membranes as a structure with a high α-helical content. A consequence of a single amino acid mutation, substitution of the Pro residue with Ala, results in an increase of membrane penetration and a higher α-helical content. The results are in accord with prior studies on the intact caveolin as well as *in silico* calculations of the preferred conformations [21].

Acknowledgements

This study was supported by the Heart and Stroke Foundation of Ontario Grant T6915 (R.M.E.). This work was also supported, in part, by the Government of Canada, by Canadian Post-Doctoral Research Fellowships 2008–09. We are grateful for Dr. Raquel F. Epand (McMaster University) with valuable discussions and suggestions and Uris Lianne Ros Quincoces (Havana University) for assistance with CD experiments.

Table 2
Secondary structure of peptides. The CD spectra were calculated the $[\theta]_{222\ nm}$, $[deg*cm^2*dmol^{-1}]$ and deconvoluted using the three programs in CDPro suite. W, WT; P, P110A; Bf, buffer; P/D/C, PO/DP/Ch. This is a representative data from experiments repeated twice. Content of secondary structure (% total).

Mixture condition	Peptide	Lipid/peptide	$-[\theta]_{222\ nm}$	α-helix	β-sheet	Turn	Random-coil
Bf.	W	(−)	4580	15.7	32.6	22.1	27.6
	P	(−)	6415	21.5	29.6	20.8	27.3
POPC in Bf.	W	10	5563	16.9	28.1	24.9	28.5
		20	4790	15.9	31.0	22.3	29.9
		40	3911	15.0	35.9	22.8	35.3
		80	4109	16.5	36.5	21.5	24.5
	P	10	7832	19.4	26.4	23.0	30.6
		20	7179	25.7	27.2	20.0	25.2
		40	7224	29.6	18.3	21.9	29.7
		80	6194	27.3	24.3	19.7	27.0
P/D/C in Bf.	W	10	5775	17.8	27.8	24.6	28.5
		20	4445	16.3	35.9	21.9	23.7
		40	3140	10.8	36.6	24.5	28.9
		80	2700	15.3	27.8	24.1	32.8
	P	10	6959	20.4	28.6	22.4	28.8
		20	5851	19.4	31.8	20.2	26.6
		40	5568	18.6	31.6	21.8	27.9
		80	3935	21.5	35.6	19.2	22.0
LPC in Bf.	W	10	7591	25.3	27.5	21.2	25.4
		20	7969	27.0	25.9	20.3	26.1
		40	7534	25.1	27.3	21.3	25.7
		80	7087	24.7	27.5	21.9	25.6
	P	10	16271	46.5	5.1	20.9	27.6
		20	17842	62.8	4.3	11.7	22.0
		40	16979	63.4	5.0	10.7	21.8
		80	13946	59.6	8.8	11.1	20.8

References

[1] R.G. Anderson, The caveolae membrane system, Annu. Rev. Biochem. 67 (1998) 199–225.
[2] A.W. Cohen, T.P. Combs, P.E. Scherer, M.P. Lisanti, Role of caveolin and caveolae in insulin signaling and diabetes, Am. J. Physiol. 285 (2003) E1151–E1160.
[3] P. Liu, M. Rudick, R.G. Anderson, Multiple functions of caveolin-1, J. Biol. Chem. 277 (2002) 41295–41298.
[4] M. Isshiki, R.G. Anderson, Function of caveolae in Ca2+ entry and Ca2+-dependent signal transduction, Traffic (Copenhagen, Denmark) 4 (2003) 717–723.
[5] M. Isshiki, R.G. Anderson, Calcium signal transduction from caveolae, Cell Calcium 26 (1999) 201–208.
[6] P. Liu, Y. Ying, Y. Zhao, D.I. Mundy, M. Zhu, R.G. Anderson, Chinese hamster ovary K2 cell lipid droplets appear to be metabolic organelles involved in membrane traffic, J. Biol. Chem. 279 (2004) 3787–3792.
[7] C.J. Fielding, P.E. Fielding, Relationship between cholesterol trafficking and signaling in rafts and caveolae, Biochim. Biophys. Acta 1610 (2003) 219–228.
[8] F. Acconcia, P. Ascenzi, A. Bocedi, E. Spisni, V. Tomasi, A. Trentalance, P. Visca, M. Marino, Palmitoylation-dependent estrogen receptor alpha membrane localization: regulation by 17beta-estradiol, Mol. Biol. Cell 16 (2005) 231–237.
[9] P. Liu, Y. Ying, R.G. Anderson, Platelet-derived growth factor activates mitogen-activated protein kinase in isolated caveolae, Proc. Natl. Acad. Sci. U.S.A. 94 (1997) 13666–13670.
[10] C. Mineo, G.L. James, E.J. Smart, R.G. Anderson, Localization of epidermal growth factor-stimulated Ras/Raf-1 interaction to caveolae membrane, J. Biol. Chem. 271 (1996) 11930–11935.
[11] J.P. Gratton, P. Bernatchez, W.C. Sessa, Caveolae and caveolins in the cardiovascular system, Circ. Res. 94 (2004) 1408–1417.
[12] T.M. Williams, F. Medina, I. Badano, R.B. Hazan, J. Hutchinson, W.J. Muller, N.G. Chopra, P.E. Scherer, R.G. Pestell, M.P. Lisanti, Caveolin-1 gene disruption promotes mammary tumorigenesis and dramatically enhances lung metastasis in vivo. Role of Cav-1 in cell invasiveness and matrix metalloproteinase (MMP-2/9) secretion, J. Biol. Chem. 279 (2004) 51630–51646.
[13] T.M. Williams, M.P. Lisanti, Caveolin-1 in oncogenic transformation, cancer, and metastasis, Am. J. Physiol. Cell Physiol. 288 (2005) C494–C506.
[14] S.B. Gaudreault, D. Dea, J. Poirier, Increased caveolin-1 expression in Alzheimer's disease brain, Neurobiol. Aging 25 (2004) 753–759.
[15] R. Hnasko, M.P. Lisanti, The biology of caveolae: lessons from caveolin knockout mice and implications for human disease, Mol. Interv. 3 (2003) 445–464.
[16] P.G. Frank, S.E. Woodman, D.S. Park, M.P. Lisanti, Caveolin, caveolae, and endothelial cell function, Arterioscler. Thromb. Vasc. Biol. 23 (2003) 1161–1168.
[17] K. Simons, R. Ehehalt, Cholesterol, lipid rafts, and disease, J. Clin. Invest. 110 (2002) 597–603.
[18] T.M. Williams, M.P. Lisanti, The caveolin proteins, Genome Biol. 5 (2004) 214.
[19] T. Okamoto, A. Schlegel, P.E. Scherer, M.P. Lisanti, Caveolins, a family of scaffolding proteins for organizing "preassembled signaling complexes" at the plasma membrane, J. Biol. Chem. 273 (1998) 5419–5422.
[20] A. Schlegel, M.P. Lisanti, A molecular dissection of caveolin-1 membrane attachment and oligomerization. Two separate regions of the caveolin-1 C-terminal domain mediate membrane binding and oligomer/oligomer interactions in vivo, J. Biol. Chem. 275 (2000) 21605–21617.
[21] S. Aoki, A. Thomas, M. Decaffmeyer, R. Brasseur, R.M. Epand, The role of proline in the membrane re-entrant helix of caveolin-1, J. Biol. Chem. 285 (2010) 33371–33380.
[22] S. Li, K.S. Song, M.P. Lisanti, Expression and characterization of recombinant caveolin. Purification by polyhistidine tagging and cholesterol-dependent incorporation into defined lipid membranes, J. Biol. Chem. 271 (1996) 568–573.
[23] A. Schlegel, R.B. Schwab, P.E. Scherer, M.P. Lisanti, A role for the caveolin scaffolding domain in mediating the membrane attachment of caveolin-1. The caveolin scaffolding domain is both necessary and sufficient for membrane binding in vitro, J. Biol. Chem. 274 (1999) 22660–22667.
[24] M. Sargiacomo, P.E. Scherer, Z. Tang, E. Kubler, K.S. Song, M.C. Sanders, M.P. Lisanti, Oligomeric structure of caveolin: implications for caveolae membrane organization, Proc. Natl. Acad. Sci. U.S.A. 92 (1995) 9407–9411.
[25] B. Christiaens, S. Symoens, S. Verheyden, Y. Engelborghs, A. Joliot, A. Prochiantz, J. Vandekerckhove, M. Rosseneu, B. Vanloo, Tryptophan fluorescence study of the interaction of penetratin peptides with model membranes, Eur. J. Biochem./FEBS 269 (2002) 2918–2926.
[26] A.H. Pande, S. Qin, K.N. Nemec, X. He, S.A. Tatulian, Isoform-specific membrane insertion of secretory phospholipase A2 and functional implications, Biochemistry 45 (2006) 12436–12447.
[27] S.S. Antollini, Y. Xu, H. Jiang, F.J. Barrantes, Fluorescence and molecular dynamics studies of the acetylcholine receptor gammaM4 transmembrane peptide in reconstituted systems, Mol. Membr. Biol. 22 (2005) 471–483.
[28] Y.M. Coic, M. Vincent, J. Gallay, F. Baleux, F. Mousson, V. Beswick, J.M. Neumann, B. de Foresta, Single-spanning membrane protein insertion in membrane mimetic systems: role and localization of aromatic residues, Eur. Biophys. J. 35 (2005) 27–39.

[29] B. de Foresta, M. Vincent, J. Gallay, M. Garrigos, Interaction with membrane mimics of transmembrane fragments 16 and 17 from the human multidrug resistance ABC transporter 1 (hMRP1/ABCC1) and two of their tryptophan variants, Biochim. Biophys. Acta 1798 (2010) 401–414.
[30] A. Chattopadhyay, E. London, Parallax method for direct measurement of membrane penetration depth utilizing fluorescence quenching by spin-labeled phospholipids, Biochemistry 26 (1987) 39–45.
[31] E. London, G.W. Feigenson, Fluorescence quenching in model membranes. 2. Determination of local lipid environment of the calcium adenosinetriphosphatase from sarcoplasmic reticulum, Biochemistry 20 (1981) 1939–1948.
[32] E. London, G.W. Feigenson, Fluorescence quenching in model membranes. 1. Characterization of quenching caused by a spin-labeled phospholipid, Biochemistry 20 (1981) 1932–1938.
[33] M.R. Eftink, C.A. Ghiron, Exposure of tryptophanyl residues in proteins. Quantitative determination by fluorescence quenching studies, Biochemistry 15 (1976) 672–680.
[34] J.R. Lakowicz, Principles of Fluorescence Spectroscopy, Third Edition Springer Science + Business Media, LLC, New York, 2006.
[35] G. Deleage, F.F. Clerc, B. Roux, ANTHEPROT: IBM PC and Apple Macintosh versions, Comput. Appl. Biosci. 5 (1989) 159–160.
[36] E. Glukhov, Y.V. Shulga, R.F. Epand, A.O. Dicu, M.K. Topham, C.M. Deber, R.M. Epand, Membrane interactions of the hydrophobic segment of diacylglycerol kinase epsilon, Biochim. Biophys. Acta 1768 (2007) 2549–2558.
[37] R.A. Melnyk, A.W. Partridge, C.M. Deber, Transmembrane domain mediated self-assembly of major coat protein subunits from Ff bacteriophage, J. Mol. Biol. 315 (2002) 63–72.
[38] R.A. Melnyk, A.W. Partridge, C.M. Deber, Retention of native-like oligomerization states in transmembrane segment peptides: application to the *Escherichia coli* aspartate receptor, Biochemistry 40 (2001) 11106–11113.
[39] C. Wang, C.M. Deber, Peptide mimics of the M13 coat protein transmembrane segment. retention of helix–helix interaction motifs, J. Biol. Chem. 275 (2000) 16155–16159.
[40] W.K. Subczynski, M. Pasenkiewicz-Gierula, R.N. McElhaney, J.S. Hyde, A. Kusumi, Molecular dynamics of 1-palmitoyl-2-oleoylphosphatidylcholine membranes containing transmembrane alpha-helical peptides with alternating leucine and alanine residues, Biochemistry 42 (2003) 3939–3948.
[41] R.A. Melnyk, A.W. Partridge, J. Yip, Y. Wu, N.K. Goto, C.M. Deber, Polar residue tagging of transmembrane peptides, Biopolymers 71 (2003) 675–685.
[42] M.R. de Planque, B.B. Bonev, J.A. Demmers, D.V. Greathouse, R.E. Koeppe II, F. Separovic, A. Watts, J.A. Killian, Interfacial anchor properties of tryptophan residues in transmembrane peptides can dominate over hydrophobic matching effects in peptide–lipid interactions, Biochemistry 42 (2003) 5341–5348.
[43] L.P. Liu, C.M. Deber, Anionic phospholipids modulate peptide insertion into membranes, Biochemistry 36 (1997) 5476–5482.
[44] A.S. Ladokhin, S. Jayasinghe, S.H. White, How to measure and analyze tryptophan fluorescence in membranes properly, and why bother? Anal. Biochem. 285 (2000) 235–245.
[45] S. Taneva, J.E. Johnson, R.B. Cornell, Lipid-induced conformational switch in the membrane binding domain of CTP:phosphocholine cytidylyltransferase: a circular dichroism study, Biochemistry 42 (2003) 11768–11776.
[46] E.A. Bryson, S.E. Rankin, M. Carey, A. Watts, T.J. Pinheiro, Folding of apocytochrome c in lipid micelles: formation of alpha-helix precedes membrane insertion, Biochemistry 38 (1999) 9758–9767.
[47] H.H. de Jongh, B. de Kruijff, The conformational changes of apocytochrome c upon binding to phospholipid vesicles and micelles of phospholipid based detergents: a circular dichroism study, Biochim. Biophys. Acta 1029 (1990) 105–112.
[48] A. Gow, W. Auton, R. Smith, Interactions between bovine myelin basic protein and zwitterionic lysophospholipids, Biochemistry 29 (1990) 1142–1147.
[49] S.E. Rankin, A. Watts, T.J. Pinheiro, Electrostatic and hydrophobic contributions to the folding mechanism of apocytochrome c driven by the interaction with lipid, Biochemistry 37 (1998) 12588–12595.
[50] J.P. Hennessey Jr., W.C. Johnson Jr., Information content in the circular dichroism of proteins, Biochemistry 20 (1981) 1085–1094.
[51] K.G. Rothberg, J.E. Heuser, W.C. Donzell, Y.S. Ying, J.R. Glenney, R.G. Anderson, Caveolin, a protein component of caveolae membrane coats, Cell 68 (1992) 673–682.
[52] E. Spisni, V. Tomasi, A. Cestaro, S.C. Tosatto, Structural insights into the function of human caveolin 1, Biochem. Biophys. Res. Commun. 338 (2005) 1383–1390.
[53] A. Karsan, J. Blonder, J. Law, E. Yaquian, D.A. Lucas, T.P. Conrads, T. Veenstra, Proteomic analysis of lipid microdomains from lipopolysaccharide-activated human endothelial cells, J. Proteome Res. 4 (2005) 349–357.
[54] R.M. Epand, B.G. Sayer, R.F. Epand, Caveolin scaffolding region and cholesterol-rich domains in membranes, J. Mol. Biol. 345 (2005) 339–350.